scientific reports

Check for updates

OPEN

circNDUFA13 stimulates adipogenesis of bone marrow-derived mesenchymal stem cells via interaction with STAT3

Longsheng Huang[1], Shan He[1], Tao Wang[1], Kai Long[1], Baicheng Ma[1], Ping Wu[1], Ying Gong[1], Donghuo Zhong[1], Qianyong Yang[1,2], Jianfang Wu[1] & Xingnuan Li[1]✉

Circular RNAs (circRNAs) in controlling gene expression have been highlighted by increasing evidence, and their dysregulation has been linked to various diseases. However, the limited role of circRNAs in the adipogenesis of bone marrow-derived mesenchymal stem cells (BMSCs) has been explored. High-throughput sequencing of circRNA was carried out on BMSCs and AD induction 7d BMSCs. Then a substantial upregulation of circNDUFA13 was detected among circRNAs in AD induction 7d BMSCs. We found that the adipogenic differentiation of BMSCs was positively linked with circNDUFA13 expression levels. Adipogenesis in BMSCs was effectively inhibited by circNDUFA13 knockdown, whereas overexpression of circNDUFA13 promoted adipogenesis. It was noted that circNDUFA13 regulated the adipogenic differentiation of BMSCs by directly interacting with the signal transducer and activator of transcription 3 (STAT3), which activates CEBPβ transcription. The in vitro model also validated the in vivo findings. our results suggest that circNDUFA13 controlled the adipogenic differentiation of BMSCs by targeting STAT3 and CEBPβ activation.

Bone marrow adipose tissue (BMAT) is a distinct type of adipose tissue that is found in the bone cavity, primarily within the bone marrow. It comprises a significant portion, up to 70%, of the total marrow space. Moreover, the process of aging exacerbates the accumulation of marrow fat within the marrow cavities[1]. It is hypothesized that BMAT originates from BMSCs found in the bone marrow stroma. Bone marrow MSCs can differentiate into multiple cell lineages, such as adipocytes, osteoblasts, etc.[2,3]. Based on the current study, patients with osteoporosis have an imbalance between BMSC adipogenic and osteogenic differentiation,with a decrease in the number of bone-forming osteoblasts and an increase in the number of marrow adipocytes[4]. A comprehensive knowledge of the cellular and molecular processes that regulate the adipogenic commitment and differentiation of BMSCs is essential for elucidating the pathogenesis of bone and metabolic diseases and identifying novel, efficient therapeutic targets.

Noncoding RNAs (ncRNAs) as regulators of adipogenic differentiation has been demonstrated by growing evidence; consequently, it is expected that they will also act as potential targets for the prevention of adipogenesis[5–7]. Besides, circular RNAs (circRNAs), classified as endogenous noncoding RNAs, originate via back-splicing of mRNA to form a covalently closed transcript. Circularization mechanisms typically categorize circRNAs into three types: intronic, exonic, and exon–intron circRNAs, which consist of both exons and introns[8]. Circular RNA is more stable than linear transcripts[9] due to its resistance to degradation by RNases and its covalently closed-loop structure; this makes circRNA a promising candidate for therapeutic targets and diagnostic biomarkers. Recently, several types of circRNAs were identified, and their functional effects in diverse biological processes (i.e., adipogenesis) have been elucidated[10,11]. However, a comprehensive understanding of the functions and mechanisms of circRNAs in adipogenesis remains unexplored.

In the present study, the circRNA expression profile was identified in BMSCs and AD induction 7d BMSCs via high-throughput sequencing. It was observed that circNDUFA13 (hsa_circ_0050243 in circBase), a circRNA

[1]Jiangxi Provincial Key Laboratory of Cell Precision Therapy, School of Basic Medical Sciences, Jiujiang University, Jiujiang 332005, Jiangxi, China. [2]Jiujiang Key Laboratory of Rare Disease ResearchSchool of Basic Medical Sciences, Jiujiang University, Jiujiang 332005, China. ✉email: 6140074@jju.edu.cn

exhibiting increased expression during adipogenic differentiation of BMSCs, possesses the ability to enhance adipogenesis in BMSCs. In light of this, the current study explored the molecular mechanism by which circNDUFA13 stimulated adipogenesis in BMSCs.

Results

Identification of circNDUFA13 in BMSCs

High-throughput sequencing was carried out on the total RNA extracted from BMSCs and AD induction 7d BMSCs. Differential expression of circRNAs was examined between the two groups, as depicted in the heat map. In the present study, a remarkable upregulation of circNDUFA13 was noted in the AD induction 7d BMSCs group (Fig. 1A). Further validation revealed that the levels of circNDUFA13 were observed to be progressively increased during the adipogenic differentiation of BMSCs, as evidenced by qPCR analysis (Fig. 1B).

The circNDUFA13 is a circular RNA molecule that originates from the NADH: ubiquinone oxidoreductase subunit A13 (NDUFA13) gene, specifically from its exon 2, 3 and 4 (Fig. 1C). Sanger sequencing analysis was performed using specific primers targeting 2 and 4 exons of circNDUFA13. The results confirmed the existence of the back splicing junction of circNDUFA13 in BMSCs, as depicted in Fig. 1D. Moreover, a set of divergent and convergent primers was specifically designed for the circNDUFA13. Both cDNA and genomic DNA (gDNA) were used as templates in BMSCs. In the findings, a 177 bp fragment was amplified using circNDUFA13 divergent primers from cDNA, yielding a single and distinct product of the anticipated size (Fig. 1E). However, no amplified product was observed from gDNA. The qPCR results indicated that circNDUFA13 exhibited RNase R resistance (Fig. 1F), whereas the circular structure of circNDUFA13 is supported by its stable property.

Further, to determine whether overexpressing or inhibiting circNDUFA13 affected the NDUFA13 expression, this study designed the following vectors: overexpression lentivirus (oe-circNDUFA13) and shRNA lentivirus (sh-circNDUFA13). The transfection of oe-circNDUFA13 resulted in a substantial upregulation of circNDUFA13 (Fig. 1G), whereas the mRNA and protein expression of NDUFA13 remained unchanged; In contrast, sh-circNDUFA13 transfection substantially lowered the level of circNDUFA13, whereas the expression of NDUFA13 mRNA and protein remained constant (Fig. 1H,I). These outcomes suggested that the modification of circNDUFA13 has no discernible effect on the expression of NDUFA13, and conversely, circNDUFA13 does not alter the expression of NDUFA13.

circNDUFA13 positively regulates BMSCs adipogenic differentiation

To examine the function of circNDUFA13 in the adipogenic differentiation of BMSCs, circNDUFA13 overexpression and knockdown were induced via transfection of BMSCs with oe-circNDUFA13, sh-circNDUFA13, and respective controls. Osteogenic differentiation was also observed in BMSCs. Furthermore, the impact of circNDUFA13 on the adipogenic potential of BMSCs was evaluated. Oil red O staining revealed that the adipogenic potential of BMSCs could be considerably reduced by knocking down circNDUFA13 while enhanced after its overexpression (Fig. 2A,B). Similarly, the expression profile of adipogenic markers was found to be substantially reduced when circNDUFA13 was knocked down but increased after its overexpression (Fig. 2C,D). These findings collectively suggest that circNDUFA13 exerts a positive impact on the regulation of adipogenic differentiation.

Upregulation of C/EBPβ level by circNDUFA13 via its interaction with STAT3

The biological functions of circRNAs are always related to the subcellular distribution. Therefore, the FISH assay was performed to determine the position of circNDUFA13, which revealed cytoplasmic and nuclear distribution of BMSCs (Fig. 3A). The results of nucleoplasmic separation experiments coupled with qPCR provided further evidence of the distribution of circNDUFA13; they indicated that circNDUFA13 is more abundant in the nucleus of BMSCs relative to the cytoplasm (Fig. 3B). This suggests that circNDUFA13 may modulate transcription by interacting with particular transcription factors, given that it is predominantly localized in the nucleus of BMSCs.

To elucidate which transcription factors interacted with circNDUFA13, the biotin-labeled RNA pulldown assay was conducted in BMSCs and adipogenic induction 7d cells using control and circNDUFA13-specific probes. Silver staining was then applied to identify the key protein partner of circNDUFA13 (Fig. 3C). The circNDUFA13 probe group comprised 33 differential proteins in BMSCs and adipogenic induction 7d cells, as identified by mass spectrometry (Supplementary Table S1). Signal transducer and activator of transcription 3 (STAT3) was one of the differential proteins that captured the interest; however, modifying the expression of circNDUFA13 had no discernible impact on the levels of STAT3 and p-STAT3 (Fig. 3D). The substantially increased level of STAT3 during adipogenic differentiation is well-known[12]. Similar findings were observed in BMSCs (Fig. 3E). The interaction between circNDUFA13 and STAT3 was also identified by the RIP PCR analysis (Fig. 3F).

Furthermore, it was found that in BMSCs, circNDUFA13 overexpression increased the expression of C/EBPβ (Fig. 4A,B). The STAT3 inhibitor stattic downregulates C/EBPβ transcriptional level during circNDUFA13 overexpression (Fig. 4C,D). Whereas circNDUFA13 knockdown reduced C/EBPβ expression. A study has revealed that STAT3 could modulate the transcription of C/EBPβ by interacting with the distal region of the C/EBPβ promoter during the early stages of adipogenesis[12]. Moreover, the ChIP experiments indicated that STAT3 binds C/EBPβ promoter, and circNDUFA13 overexpression enhanced this binding ability of STAT3 in BMSCs (Fig. 4E,F).

In vivo, the knockdown of circNDUFA13 impeded the adipogenic differentiation of preadipocytes

To evaluate the possible impact of circNDUFA13 on adipogenesis in vivo, BMSCs were induced in an adipogenic medium for 5 days after being transfected with a particular lentivirus (sh-control, sh-circNDUFA13, oe-control, or oe-circNDUFA13). The transfected cells were then mixed with Matrigel and injected subcutaneously into nude

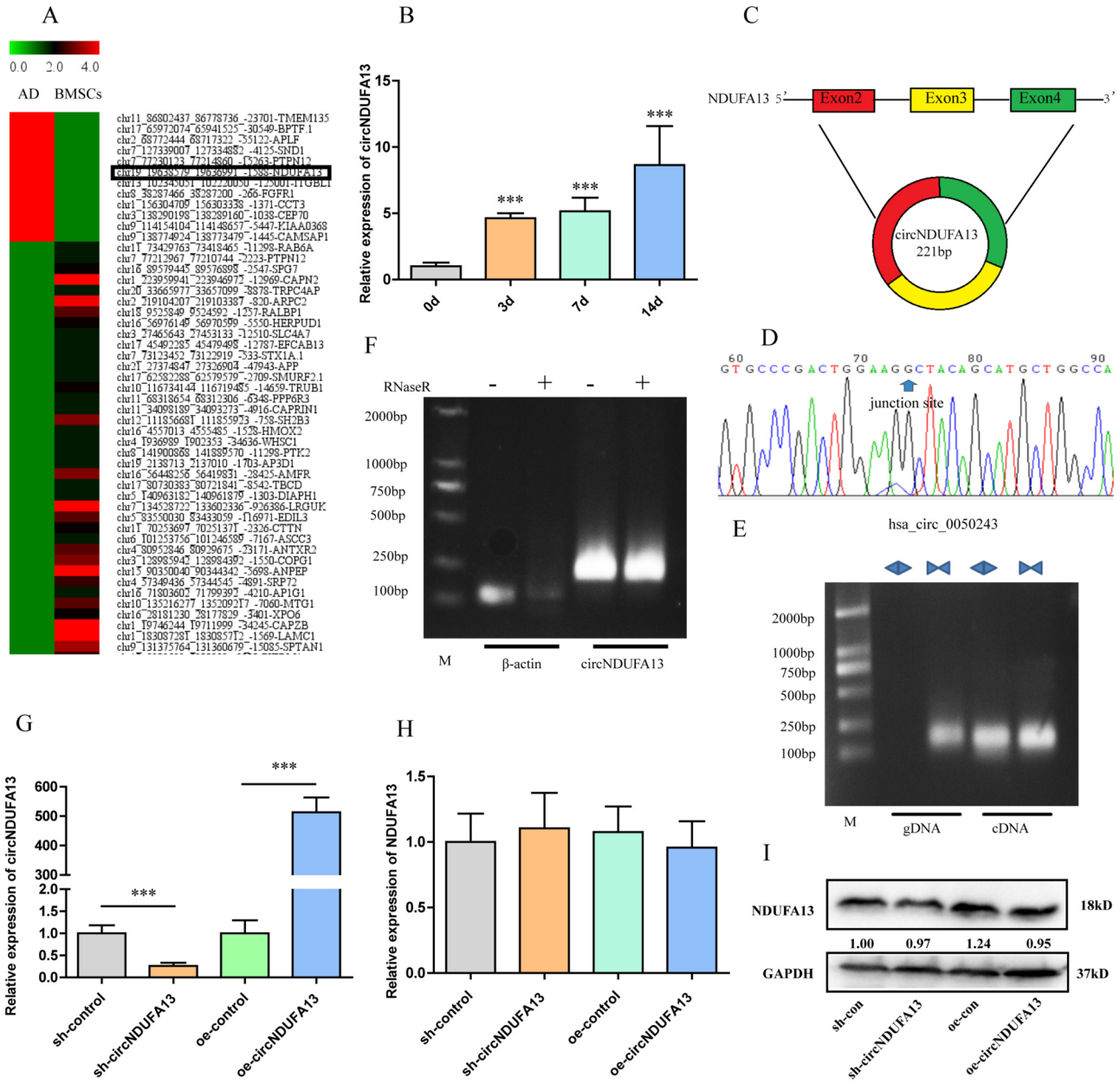

Fig. 1. Detection and validation of circNDUFA13 in BMSCs. (**A**) Heatmap displayed differentially expressed circRNAs between BMSCs and AD induction 7d BMSCs. Upregulated circRNAs are denoted by red, while downregulated circRNAs are represented by green. (**B**) Expression levels of circNDUFA13 were measured by qPCR at different time points during adipogenic differentiation. (**C**) The circular NDUFA13 originated schematically from exons 1–3 of the NDUFA13 gene. (**D**) Head-to-tail splicing was validated by using Sanger sequencing. (**E**) The circCAPRIN1 was identified via divergent and convergent primers derived from cDNA and gDNA. (**F**) Expression of circNDUFA13 was measured by RT-PCR treated with RNase R, and β-actin was used as a reference gene or negative control. (**G**, **H**) Relative expression of circNDUFA13 (**G**) and NDUFA13 (**H**) was detected by qPCR after overexpression or downexpression circNDUFA13. (**I**) Protein expression levels of DUFA13 in BMSCs after circNDUFA13 overexpression or down expression. Gels/blots were cropped from different regions of the same gel and are delineated by clear dividing lines. (Note: for (**I**) the original blots/gels are presented in Supplementary Fig. S1; for (**E**, **F**) the original blots/gels are presented in Supplementary Fig. S5).

mice (Fig. 5A). After 8 weeks, the preadipocytes/Matrigel plugs were extracted, and adipocytes were identified via H&E.

In the findings of H&E staining, the sh-circNDUFA13 group comprised considerably fewer adipocytes than the sh-control group (Fig. 5B). In contrast, the oe-circNDUFA13 group contained a larger amount of adipocytes than the oe-control group.

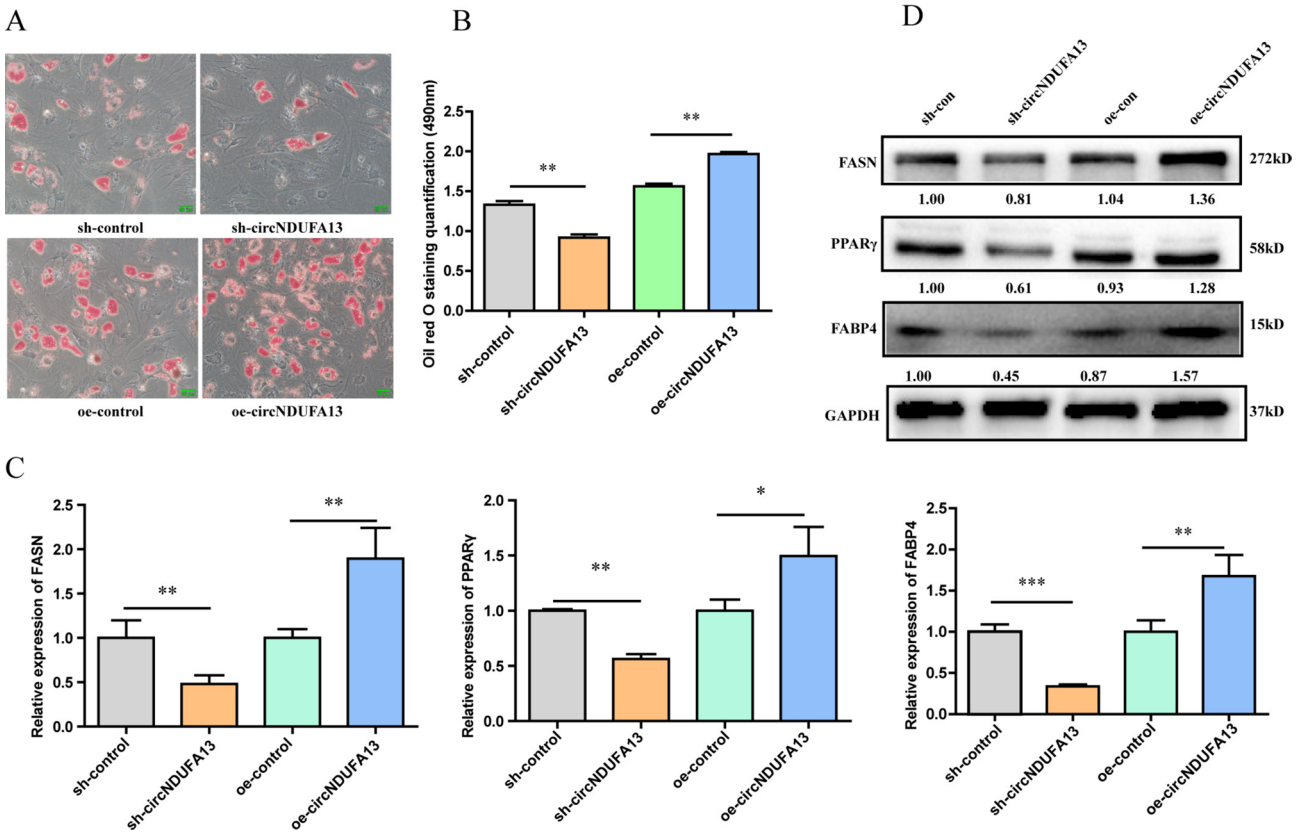

Fig. 2. CircNDUFA13 affected adipogenic differentiation of BMSCs. (**A**, **B**) Lipid droplet deposition was detected through oil O staining (**A**) and quantitation (**B**). (20X; scale bar = 20 μm). The results of three independent/separate experiments are displayed as the mean ± SD. (**C**) The mRNA levels of PPARγ, FASN, FABP4 were measured by qPCR (*** $p \leq 0.001$; ** $p \leq 0.01$; * $p \leq 0.05$). (**D**) The levels of protein expression for FASN, PPARγ, and FABP4 were determined in cell lysates. Different gels were used, and blots were combined for presentation, with clear delineations between them. (Note: for (**D**) the original blots/gels are presented in Supplementary Fig. S2).

Overall, adipogenesis was impaired in vivo when circNDUFA13 was knocked down in preadipocytes derived from BMSCs; conversely, circNDUFA13 overexpression facilitated adipogenesis in vivo, confirming the in vitro observations.

Discussion

Adipocyte formation is generally dysregulated, leading to multiple diseases, including atherosclerosis, obesity, fatty liver, diabetes, and osteoporosis. For instance, osteoporosis is strongly associated with bone marrow adipose tissue accumulation, which occurs naturally with age and in metabolic disorders[13,14].

Adipose development is controlled by multiple intricate processes, as proven by a substantial number of experiments. Among these processes, circRNAs have emerged as significant contributors to the regulation of adipocyte differentiation. Adipocyte differentiation-related circRNAs have been identified in multiple studies. One of the few studies demonstrated that the suppression of hsa_circH19 leads to improved adipogenic differentiation in human adipose-derived stem cells (hADSCs) by specifically targeting PTBP1[15]. As a result, the expression of hsa_circH19 may be associated with lipid metabolism in adipose tissue affected by metabolic syndrome. In another study, it was discovered that circMAPK9 functioned as a ceRNA by sequestering has-miR-1322. This interaction resulted in a reduction in the inhibitory impact on fat mass and obesity-related protein, ultimately facilitating adipogenesis[16].

All the studies mentioned above validated the regulatory impact of circRNAs on adipogenic differentiation in hADCSs and adipose tissue. To determine whether circRNA is implicated in the osteoporosis development and adipogenic differentiation of BMSCs. This will be an interesting question to be explored. In this study, the circNDUFA13 was found to be elevated in BMSCs during adipogenic differentiation. Adipogenesis of BMSCs was inhibited by circNDUFA13 knockdown, whereas overexpression of circNDUFA13 caused the opposite effect, indicating that circNDUFA13 is essential for the adipogenic differentiation of BMSCs.

The present study provides the confirmatory role of circRNA in adipogenic differentiation of BMSCs. Then what is the regulatory mechanism of circRNA? The biological functions of circRNAs are known to be mediated via three distinct mechanisms[17]. First, by binding to miRNAs, circular RNAs function as sponges that control miRNA activities. Second, they facilitate the translation of encoded proteins or modulate gene expression at the

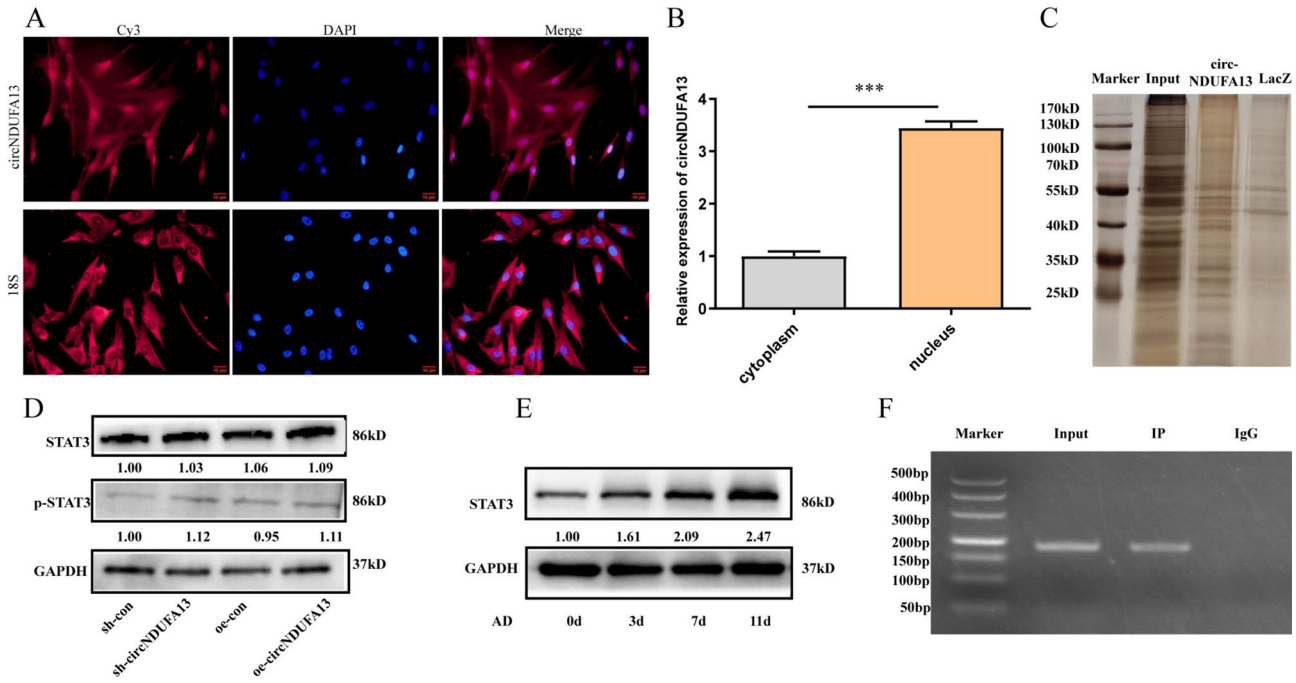

Fig. 3. Localization of circNDUFA13 and validation of interaction between circNDUFA13 and STAT3. (**A**, **B**) Localization of circNDUFA13 was explored in BMSCs through FISH and nucleoplasmic separation experiments. (**C**) Silver staining and mass spectrometry were carried out after the RNA pull-down assay was obtained with the specific biotin-labeled circNDUFA13 probe in BMSCs. (**D**) Protein expression levels of STAT3 and p-STAT3 in BMSCs after circNDUFA13 overexpression or down expression. Different gels were used, and blots were combined for presentation, with clear delineations between them. (**E**) Protein expression levels of STAT3 in BMSCs at different time points during adipogenic differentiation. Gels/blots were cropped from different regions of the same gel and are delineated by clear dividing lines. (**F**) The enrichment of RNA was identified by PCR after a RIP assay was conducted on BMSCs using anti-STAT3 or anti-IgG. (Note: for (**D**, **E**) the original blots/gels are presented in Supplementary Fig. S3; for (**C**, **F**) the original blots/gels are presented in Supplementary Fig. S6).

levels of splicing and transcription[18–21]. Third, the regulatory mechanisms of circRNA are intricately linked to the subcellular distribution of RNA molecules[22].

The findings revealed that circNDUFA13 is predominantly localized in the nucleus of BMSCs (Fig. 3A,B). However, cytoplasmic expression is comparatively low, indicating that its function may be primarily confined to the nucleus. So can the small amount of circNDUFA13 distributed in the cytoplasm be translated? Studies found that the translation of circRNAs is different from mRNA, and is cap-independent translation, initiated by IRES (Internal Ribosome Entry site) or m6A modified structure[23,24]. We used ORFfinder (https://www.ncbi.nlm.nih.gov/orffinder/), circBank (http://www.circbank.cn/index.html) and circAtlas (https://ngdc.cncb.ac.cn/circatlas/) to detect ORF, IRES and m6A site in circNDUFA13, and the results showed that there are ORFs, but no IRES or m6A site were found. Thus, circNDUFA13 can not be translated. Generally, circRNAs can control adipogenesis via multiple processes; however, their most prevalent form involves their localization in the cytoplasm of the cell and their function as microRNA sponges[25]. Thus, this study may provide a comprehensive understanding of how circRNAs exert their biological effects on adipogenesis.

RNA pull-down experiments and RIP assays were carried out to identify proteins that might interact with circNDUFA13; the outcomes suggested that STAT3 was a downstream target of circNDUFA13. Concurrently, the STAT3 level was quantified, and the expression of circNDUFA13 did not exhibit any clear effect on the STAT3 levels (Fig. 3D). Thus, it was suggested that circNDUFA13 might influence the function of STAT3 to regulate the transcription of target genes.

Previous studies have demonstrated that STAT3 can interact with the promoter regions of genes associated with adipogenesis, such as C/EBPβ, thereby promoting their expression[12,26]. This finding provides substantial evidence in favor of the resultant outcomes. During adipogenesis, C/EBPβ, a member of the C/EBP family, is an essential regulator of gene expression[27,28]. The occupancy of STAT3 in the promoter of C/EBPβ was confirmed via ChIP assays. Further, the PCR results indicated that the presence of circNDUFA13 affected STAT3 interaction with the promoter of C/EBPβ (Fig. 4E,F). However, this study has provided evidence for the interaction between circNDUFA13 and STAT3 and its consequential impact on the transcriptional regulatory function of STAT3 on C/EBPβ. This finding further substantiates that circRNAs can modulate transcriptional levels by interacting with transcription factors. Based on these promising outcomes with BMSCs, cells (circNDUFA13-overexpressing and knocking down BMSCs) were injected subcutaneously into nude mice to determine whether circNDUFA13 can inhibit adipocyte formation in vivo. The formation of lipid droplets was subsequently observed to be increased

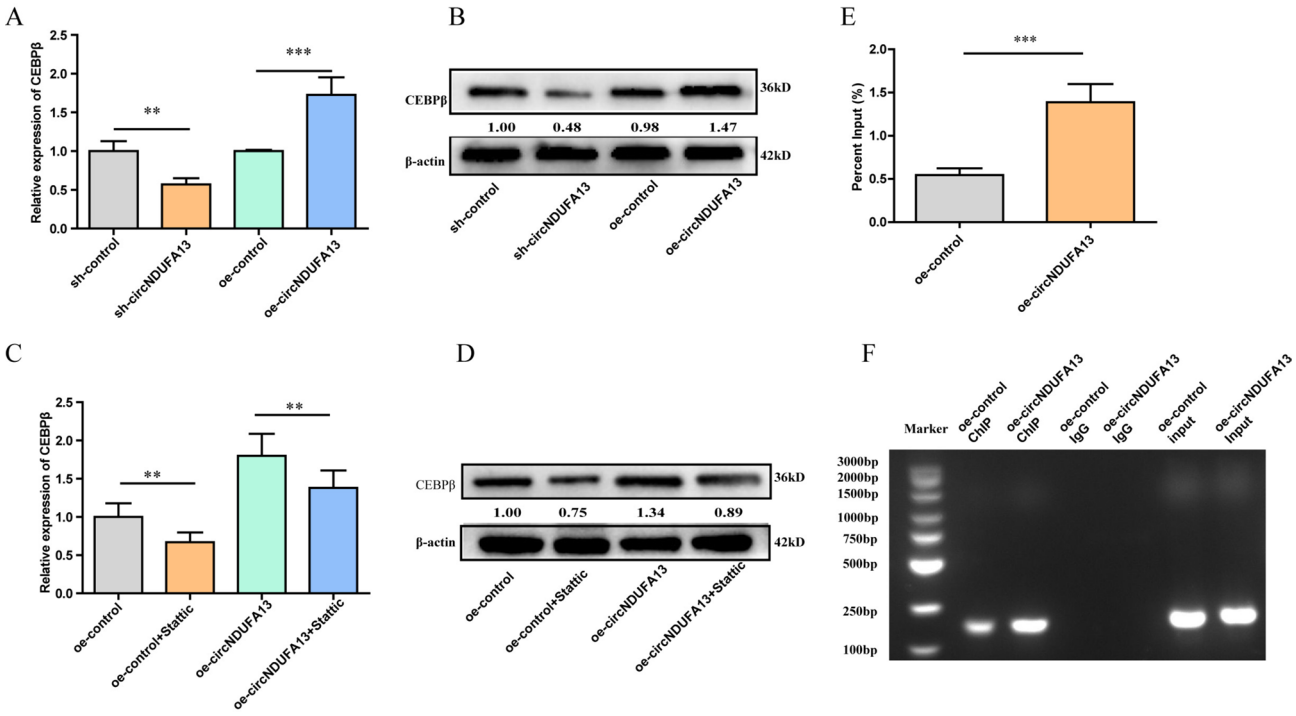

Fig. 4. Activation of STAT3 by circNDUFA13 induces CEBPβ transcription. (**A**) The CEBPβ expression levels in BMSCs were monitored after circNDUFA13 overexpression or down expression using qPCR. (**B**) The protein expression levels of CEBPβ in BMSCs were monitored after circNDUFA13 overexpression or down expression using western blot**.** Gels/blots were cropped from different regions of the same gel and are delineated by clear dividing lines. (**C**) The CEBPβ expression levels in BMSCs were monitored after STAT3 was inhibited using qPCR. (**D**) The protein expression levels of CEBPβ in BMSCs were monitored after STAT3 was inhibited using western blot**.** Gels/blots were cropped from different regions of the same gel and are delineated by clear dividing lines. (**E**, **F**) Enhanced STAT3 interaction with the promoter region of CEBPβ in BMSCs after transfection with circNDUFA13, as determined by RT-qPCR results of ChIP analysis, (**E**) the percent of CEBPβ promoter between oe-circNDUFA13 and oe-control and (**F**) the agarose gel electrophoresis image. (Note: for (**B**, **D**) the original blots/gels are presented in Supplementary Fig. S4; for (**F**) the original blots/gels are presented in Supplementary Fig. S7).

and decreased, respectively. As suggested by these results, circNDUFA13 may also be involved in the progression of osteoporosis and is a key target in the adipocyte formation of BMSCs.

The study concluded that circNDUFA13, a circRNA that is elevated during BMSCs adipogenic differentiation, can stimulate BMSCs adipogenesis for the first time. Besides, circNDUFA13 facilitates CEBPβ transcription, which is associated with adipogenic differentiation, via interaction with the STAT3 protein. Thus, a novel perspective on the function of circNDUFA13 is provided by this regulatory mechanism. In addition to shedding light on the mechanism of bone metabolism disorders like osteoporosis, these outcomes indicated that circNDUFA13 could be a novel therapeutic target for BMSCs, thereby enhancing their clinical applications.

Material and methods

Cell propagation and differentiation

Cells (BMSCs) were isolated from the bone marrow of young and healthy individuals who did not exhibit any signs of osteoporosis. Informed consent was obtained from all volunteers. The present study was approved by the Ethics Committee of Medical School of Jiujiang University (approval number: JJU20230009) and all experiments were performed in accordance with relevant guidelines and regulations. Following passage 5, flow cytometry was used to confirm that about ≤ 95% of the isolated BMSCs were positive for CD90, CD73, and CD105 markers. The results indicated that approximately 5% of the cell population exhibited positive expression for CD HLA-DR, CD19, CD34, and CD45 biomarkers. The cell culture procedure was carried out by using an OriCell BMSC growth medium (HUXMA-90011, enriched with glutamine, penicillin, streptomycin, and 10% FBS). After suspending 5 × 104 cells in the defined culture medium, the cells were maintained in a controlled culture environment with 5% CO2. Adipogenic cocktails were employed to stimulate adipogenesis; these cocktails comprised dexamethasone, 3-isobutyl-1-methylxanthine (0.5 mM each), insulin (10 µg/ mL), and 10% FBS. Each chemical used in this study was procured from Gibco, US. The differentiation was induced and maintained for 3–7 days, during which the culture media was replaced with fresh media every 3 days. The Oil Red O staining was used to detect the lipid droplets in the differentiated cells on day 7 of the experimental procedure. The mRNA and protein concentrations of these cells (red) were quantified on days 3 and 7.

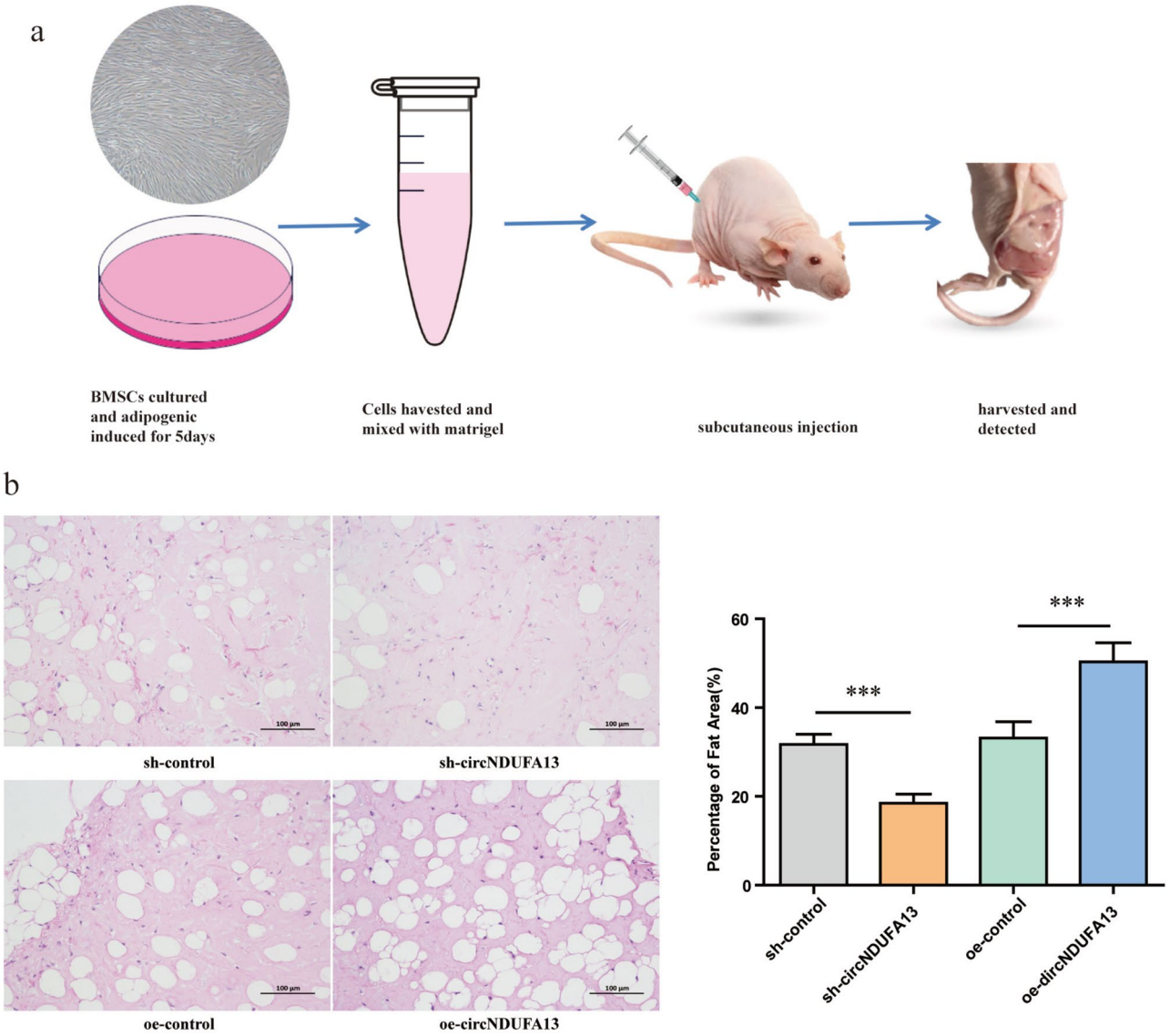

Fig. 5. In vivo effect of circNDUFA13 on preadipocyte adipogenic differentiation. (**A**) Representation of the in vivo experimental design. Before in vivo transplantation, BMSCs were transfected with lentiviruses (sh-control, sh-circNDUFA13, oe-control, and oe-circNDUFA13) and adipogenesis was stimulated for 5 days. Differentiated cells were collected and mixed with Matrigel, which was transplanted subcutaneously into the space of nude mice and monitored after 8 weeks. (**B**) An analysis of H&E staining revealed a reduced number of adipocytes in the sh-circNDUFA13 group relative to the sh-control group, while the oe-circNDUFA13 group comprised a higher percentage of adipocytes. (Scale bar = 100 mm).

RNA fluorescence in situ hybridization (FISH)

RiboBio (RiboBio Biotechnology, China) designed circNDUFA13 and 18S probes that were labeled with Cy3. Hybridization was carried out for 12 h in a humidified chamber at 37 °C. The signals produced by circNDUFA13 were identified as per the manufacturer's guidelines using a FISH kit (RiboBio, China). All fluorescence images were acquired via an Olympus IX73 microscope.

Biotin-labeled RNA pulldown

Control and circNDUFA13 probes with biotin labels were designed by BersinBio Biotechnology (Supplementary Table S3). Biotin-labeled RNA pulldown was conducted via the RNA Pulldown Kit (BersinBio, China) in line with the manual's guidelines. Precisely, the probes were kept with streptavidin-coated magnetic beads at 25 °C for 30 min. In the lysis buffer, cells were lysed, and their nucleic acid was extracted from the lysates and incubated with probe-bound magnetic beads for 2 h at 25 °C. This probe-bead-protein complex was subsequently rinsed four times with washing buffer. The extraction of the binding proteins within the complex was carried out. These proteins were detected by SDS-PAGE and subsequently stained with the Fast Silver Stain Kit (P0017S; Beyotime) as per the manufacturer's instructions. The specific proteins were subsequently identified using mass spectrometry (BersinBio, China).

RNA immunoprecipitation (RIP)

The interaction between circNDUFA13 and STAT3 protein was validated using an RIP Kit (BersinBio, Bes5101, China). Briefly, magnetic beads were treated with 5 μg of antibodies (anti-STAT3 (CST, 9139S, USA) and anti-immunoglobulin G (IgG) (Millipore, USA) for 30 min at 25 °C. The lysate of 2 × 107 cells was incubated at 4 °C overnight with antibody-coated magnetic beads. After six washes with RIP washing buffer, the bead-protein-RNA complexes were kept with proteinase K digestion buffer and rotated at 55 °C for 1 h. Following the extraction and reverse transcription of RNA to cDNA, the concentration of circNDUFA13 was measured via qPCR and normalized to the input.

Cell transfection

Short hairpin RNAs lentiviral vectors targeting circNDUFA13 (sh-circNDUFA13), overexpression lentiviral vectors for circNDUFA13 (oe-circNDUFA13) and control vectors were synthesized by Genechem Co., Ltd. (Shanghai, China). The transfection efficiency was evaluated using a lentivirus-encoded green fluorescence protein (GFP). Cells (BMSCs) were allowed to grow into 6-well plates until they reached 20–30% confluency. After culturing, 10 μL of lentivirus with 1 × 108 TU/mL titer was added to each well, along with 5 μg/mL of polybrene in complete media. Following incubating for 10 h, the media was changed with fresh media, and the cells were further maintained for 72 h.

Isolation of nuclear and cytoplasmic fractions

The extraction of cytoplasmic and nuclear RNA was carried out in line with the manual's instructions via Thermo Fisher BioReagents (Cat #AM1921). Precisely, to separate the nuclear fraction from the cytoplasmic fraction, the cells were harvested, lysed with cell fraction buffer, and centrifuged at a low speed. Following this, the nuclear pellet was carefully isolated from the cytoplasmic fraction, and the cell disruption reagent was added to the nuclear pellet. RNA isolation was performed on the samples according to the manufacturer's guidelines.

Chromatin immunoprecipitation (ChIP) assay

This assay was conducted based on the protocol outlined by the manufacturer (Millipore, USA). Formaldehyde was used to cross-link the cells, which were then terminated by incubation with glycine. After sonicating chromatin with a sonication buffer, it was incubated overnight with rabbit IgG or anti-STAT3 antibody. The DNA fragments were purified via phenol–chloroform extraction. Subsequently, the RT-qPCR was performed to analyze the samples. Supplementary Table S2. 1 contains a list of primers for the C/EBPβ promoter region.

Oil red O staining and lipid quantification

Initially, cells were rinsed with PBS at respective time points before being fixed at 25 °C for 30 min using 4% formalin. The cells were washed twice with PBS, followed by a 30-min staining period with 60% saturated Oil Red O. The cells were again washed twice before microscopic examination (Olympus IX73, Japan). The dye was removed from the cells using isopropanol after imaging. The level of intracellular lipid droplet formation was quantified using an absorbance at 490 nm determined by a microplate reader (Biorad iMARK, USA).

Gene expression analysis

Total RNA extraction was carried out using Trizol (Invitrogen, USA) based on the recommended protocol. For cDNA synthesis, a Reverse Transcription System and Oligo (dT) (Thermo Scientific, USA) were used. The defined primers were designed by RiboBio (Guangzhou, China) as shown in the provided Supplementary Table S2. The expression of β-actin mRNA was used as a control for the normalization of circRNA and mRNAs. For qRT-PCR reactions, a 7500 Real-Time PCR System (ABI, USA) was used in combination with an SYBR Premix Ex Taq reagent (TOYOBO, Japan). Data was measured using the 2-ΔΔCT method.

Western blotting

Cells were harvested on ice using RIPA buffer. The lysates were boiled in 5X SDS sample buffer for 5 min. All proteins were subjected to SDS-PAGE and transferred onto PVDF membranes (Millipore, USA), which were then cut into pieces based on the molecular size of the target proteins. These membranes (blots) were blocked with non-fat milk and probed with primary rabbit antibodies against PPARγ (1:1000; 2435, CST), FASN (1:1000; 10624-2-AP; Proteintech), C/EBPβ (1:1000; 23431-1-AP; Proteintech), FABP4 (1:1000; 12802-1-AP; Proteintech), STAT3 (1:1000; 10253-2-AP; Proteintech), p-STAT3 (1:1000; 9145; Cell signaling) GAPDH (1:2000; 60004-1-AP; Proteintech) and β-actin (1:2000; 20536-1-AP; Proteintech). The anti-rabbit HRP-linked IgG secondary antibody (1:10000; SA00001-2; Proteintech) was used to detect protein bands on blots, visualized by chemiluminescence.

Preadipocytes adipogenic differentiation in vivo

The procedure for conducting this experiment was outlined in a previous study[29]. Following in vitro transfection of BMSCs with the lentivirus (sh-control, sh-circNDUFA13, oe-control and oe-circNDUFA13), the cells were incubated for 5 days in adipogenic differentiation medium. These transfected cells were mixed with Matrigel (200 μL) (BD Biosciences, USA) and subcutaneously transplanted to the back of 8-week-old BALB/c-nu/nu female nude mice (three mice/group) (Mice were purchased form Laboratory Animal Tech of Hangzhou Ziyuan, China). All animal experiments were conducted according to protocols approved by the Animal Care and Use Committee of Medical School of Jiujiang University (approval number: JJU20230020). The cells/Matrigel implants were collected after 8 weeks and fixed for 24 h using 4% paraformaldehyde. After decalcification, embedding, and

slicing of the implants, hematoxylin, and eosin (H&E) staining was performed. All animal experiments were reported in accordance with ARRIVE guidelines.

H&E staining

All tissue sections were deparaffinized in xylene and hydrated in a series of ethanol concentrations. The sections were stained with hematoxylin for 5 min, followed by 3 min of eosin staining after clearing. Following the staining, progressively increased concentrations of xylene and ethanol were used to dehydrate each section. All sections were visualized under a light microscope.

Statistical analysis

Data was analyzed in the form of the mean ± standard deviation (SD) ($x \pm s$). The disparities were examined using GraphPad Prism 7.5. To examine the variations between the two groups, the Student's t-test was applied. 2. A post hoc analysis of variance using one-way ANOVA with Tukey's test was applied to examine the differences between three or more groups. The value of $p \leq 0.05$ was selected to define the significance level. The circRNAs that exhibited differential expression were identified by a p-value ≤ 0.05 and a fold change ≥ 2.

Data availability

The data set used and/or analyzed in the current research can be obtained from the corresponding author upon reasonable request.

Received: 30 January 2024; Accepted: 22 August 2024
Published online: 26 August 2024

References

1. Fazeli, P. K. *et al.* Marrow fat and bone—New perspectives. *J. Clin. Endocrinol. Metab.* **98**, 935–945 (2013).
2. van Staa, T. P., Leufkens, H. G. & Cooper, C. The epidemiology of corticosteroid-induced osteoporosis: A meta-analysis. *Osteoporos Int.* **13**, 777–787 (2002).
3. Bredella, M. A. *et al.* Increased bone marrow fat in anorexia nervosa. *J. Clin. Endocrinol. Metab.* **94**, 2129–2136 (2009).
4. Moerman, E. J., Teng, K. & Lipschitz, D. A. Lecka-Czernik B Aging activates adipogenic and suppresses osteogenic programs in mesenchymal marrow stroma/stem cells: The role of PPARgamma2 transcription factor and TGF-beta/BMP signaling pathways. *Aging Cell* **3**, 379–389 (2004).
5. Hamam, D. *et al.* microRNA-320/RUNX2 axis regulates adipocytic differentiation of human mesenchymal (skeletal) stem cells. *Cell Death Dis.* **5**(10), e1499 (2014).
6. Cooper, D. R. *et al.* Long non-coding RNA NEAT1 associates with SRp40 to temporally regulate PPARγ2 splicing during adipogenesis in 3T3-L1 cells. *Genes (Basel).* **5**(4), 1050–1063 (2014).
7. Dong, M. J. *et al.* MicroRNA 182 is a novel negative regulator of adipogenesis by targeting CCAAT/enhancer-binding protein α. *Obesity (Silver Spring).* **28**(8), 1467–1476 (2020).
8. Gao, Y. *et al.* Comprehensive identification of internal structure and alternative splicing events in circular RNAs. *Nat. Commun.* **7**, 12060 (2016).
9. Wang, Z. *et al.* Circular RNAs: Biology and clinical significance of breast cancer. *RNA Biol.* **20**(1), 859–874 (2023).
10. Lin, Z. J. *et al.* Functions and mechanisms of circular RNAs in regulating stem cell differentiation. *RNA Biol.* **18**(12), 2136–2149 (2021).
11. Yang, L., Wilusz, J. E. & Chen, L. L. Biogenesis and regulatory roles of circular RNAs. *Annu. Rev. Cell Dev. Biol.* **38**, 263–289 (2022).
12. Zhang, K., Guo, W., Yang, Y. & Wu, J. JAK2/STAT3 pathway is involved in the early stage of adipogenesis through regulating C/EBPβ transcription. *J. Cell Biochem.* **112**(2), 488–497 (2011).
13. Boroumand, P. & Klip, A. Bone marrow adipose cells—Cellular interactions and changes with obesity. *J. Cell Sci.* **133**(5), jcs238394 (2020).
14. Beekman, K. M. *et al.* Osteoporosis and bone marrow adipose tissue. *Curr. Osteoporos Rep.* **21**(1), 45–55 (2023).
15. Zhu, Y. Y., Gui, W., Lin, X. & Li, H. Knock-down of circular RNA H19 induces human adipose-derived stem cells adipogenic differentiation via a mechanism involving the polypyrimidine tract-binding protein 1. *Exp. Cell Res.* **387**(2), 111753 (2020).
16. Chen, S. *et al.* CircMAPK9 promotes adipogenesis through modulating hsa-miR-1322/FTO axis in obesity. *Science.* **26**(10), 107756 (2023).
17. Zhou, W. Y. *et al.* Circular RNA: Metabolism, functions and interactions with proteins. *Mol. Cancer.* **19**(1), 172 (2020).
18. Panda, A. C. Circular RNAs act as miRNA sponges. *Adv. Exp. Med. Biol.* **1087**, 67–79 (2018).
19. Xiong, L. *et al.* A novel protein encoded by circINSIG1 reprograms cholesterol metabolism by promoting the ubiquitin-dependent degradation of INSIG1 in colorectal cancer. *Mol. Cancer.* **22**(1), 72 (2023).
20. Eger, N., Schoppe, L., Schuster, S., Laufs, U. & Boeckel, J. N. Circular RNA splicing. *Adv. Exp. Med. Biol.* **1087**, 41–52 (2018).
21. Yang, Y. *et al.* circCAPRIN1 interacts with STAT2 to promote tumor progression and lipid synthesis via upregulating ACC1 expression in colorectal cancer. *Cancer Commun. (Lond).* **43**(1), 100–122 (2023).
22. Liu, C. X. & Chen, L. L. Circular RNAs: Characterization, cellular roles, and applications. *Cell.* **185**(12), 2016–2034 (2022).
23. Diallo, L. H. *et al.* How are circRNAs translated by non-canonical initiation mechanisms?. *Biochimie.* **164**, 45–52 (2019).
24. Shi, Y., Jia, X. & Xu, J. The new function of circRNA: translation. *Clin. Transl. Oncol.* **22**(12), 2162–2169 (2020).
25. Ru, W. X. *et al.* Non-coding RNAs and adipogenesis. *Int. J. Mol. Sci.* **24**(12), 9978 (2023).
26. Wu, R. F. *et al.* m6A methylation modulates adipogenesis through JAK2-STAT3-C/EBPβ signaling. *Biochim. Biophys. Acta Gene Regul. Mech.* **1862**(8), 796–806 (2019).
27. Zanotti, S., Stadmeyer, L., Smerdel-Ramoya, A., Durant, D. & Canalis, E. Misexpression of CCAAT/enhancer binding protein beta causes osteopenia. *J. Endocrinol.* **201**(2), 263–274 (2009).
28. Guo, L., Li, X. & Tang, Q. Q. Transcriptional regulation of adipocyte differentiation: A central role for CCAAT/enhancer-binding protein (C/EBP) β. *J. Biol. Chem.* **290**(2), 755–761 (2015).
29. Zhang, Y. H. *et al.* Impairment of APPL1/Myoferlin facilitates adipogenic differentiation of mesenchymal stem cells by blocking autophagy flux in osteoporosis. *Cell Mol. Life Sci.* **79**(9), 488 (2022).

Author contributions

LXN and HLS conceived and designed the study. HLS, WT, HS, and LK performed the experiments. MBC, ZDH, GY and WP performed the data analyses and manuscript preparation. HLS,YQY and WJF wrote the manuscript

with input from all co-authors. LXN and WT revised the manuscript. All authors read and approved the fnal manuscript.

Funding
This study was funded by National Natural Science Foundation of China (81960411, 8410200, 82360443, 82360177), Key Project of Jiangxi Provincial Natural Science Fundation (20224ACB206011) and Natural Science Foundation of Jiangxi Province, China (20232BAB206051).

Competing interests
The authors declare no competing interests.

Additional information
Supplementary Information The online version contains supplementary material available at https://doi.org/10.1038/s41598-024-70867-9.

Correspondence and requests for materials should be addressed to X.L.